

The ROSAT all-sky survey catalogue of optically bright late-type giants and supergiants^{*}

M. Hünsch^{1,2}, J.H.M.M. Schmitt¹, and W. Voges¹

¹ Max-Planck-Institut für Extraterrestrische Physik, Giessenbachstr., 85740 Garching, Germany

² Hamburger Sternwarte, Gojenbergsweg 112, 21029 Hamburg, Germany

Received March 26; accepted May 5, 1997

Abstract. We present X-ray data for all late-type (A, F, G, K, M) giants and supergiants (luminosity classes I to III-IV) listed in the Bright Star Catalogue that have been detected in the ROSAT all-sky survey. Altogether, our catalogue contains 450 entries of X-ray emitting evolved late-type stars, which corresponds to an average detection rate of about 11.7 percent. The selection of the sample stars, the data analysis, the criteria for an accepted match between star and X-ray source, and the determination of X-ray fluxes are described.

Key words: stars: activity — stars: coronae — stars: late-type — X-rays: stars — catalogs

1. Introduction

Late-type stars are among the most frequent classes of X-ray sources. As suggested by the study of the Sun, their X-ray emission is believed to be thermal emission from hot (10^6 K) coronal plasma. Hundreds of late-type stars were already detected by the *Einstein* and EXOSAT Observatories (cf. Vaiana et al. 1981) with X-ray luminosities mostly ranging from about solar level (i.e., 10^{27} erg s⁻¹) up to $\sim 10^{31}$ erg s⁻¹. Recent ROSAT observations of a complete sample of the nearest stars (Schmitt et al. 1995; Schmitt 1997) have demonstrated that virtually all late-type main-sequence stars are X-ray sources. It is generally accepted that the existence of outer convection zones (starting at late A-types) as well as rotation are essential conditions for magnetically heated stellar coronae. A relation between X-ray luminosity and rotation velocity was first established by Pallavicini et al. (1981), and gave

an incentive for numerous further studies in the context of the rotation-activity relationship. In connection with angular momentum evolution stellar X-ray emission can thus be regarded as a rough age-indicator.

Contrary to main-sequence stars, not all late-type giants and supergiants were found as X-ray sources. In particular, IUE and *Einstein* observations suggested that in certain regions of the Hertzsprung-Russell (HR) diagram late-type giants possess hot transition regions and coronae while in other regions such hot material is absent. The boundary between these different regions in the HR diagram is indicated by several dividing lines based on different observational criteria (cf. Linsky & Haisch 1979; Ayres et al. 1981; Haisch et al. 1991, 1992). Sensitive new ROSAT observations have substantially revised this picture. While Hünsch et al. (1996a) have shown from a complete, volume-limited sample that probably all but the very latest giants are X-ray sources of mostly about solar level, Reimers et al. (1996) detected X-ray emission from several bright giants and supergiants (the so-called hybrid stars) obviously violating the strict dividing line concept. Recently, Hünsch & Schröder (1996) suggested a scenario in which the observed coronal properties of late-type giants and supergiants can be qualitatively understood in the context of stellar and angular momentum evolution.

It is obvious that all such investigations are severely hampered by the scarcity of X-ray detected evolved stars. A compilation of the *Einstein* detections is given by Maggio et al. (1990) and includes 69 detected giants and supergiants of spectral types F to M. Additionally, for 310 such stars upper limits of X-ray emission were derived. However, we have to keep in mind that the *Einstein* observations only covered about 10% of the sky with rather inhomogeneous exposure times. The Maggio et al. data consist of both pointed observations on individual stars and serendipitous observations in the field-of-view of other targets.

Contrary to the *Einstein* observations, the ROSAT observatory scanned the whole sky during the first half year of its mission. The ROSAT all-sky survey (RASS) resulted

Send offprint requests to: M. Hünsch, e-mail: mhunsch@rosat.mpe-garching.mpg.de

^{*} Catalogue only available at CDS via anonymous ftp to cdsarc.u-strasbg.fr (130.79.128.5) or via <http://cdsweb.u-strasbg.fr/Abstract.html>

in about 150 000 detected X-ray sources, which form a flux-limited but otherwise unbiased sample (Voges et al. 1996a).

We have searched for X-ray detections of optically bright late-type giants and supergiants in the RASS data. The aim of this paper is to provide the X-ray data of those detections in the form of a homogeneous catalogue. We describe the way the catalogue was created and how the X-ray properties of the stars were derived. For a detailed astrophysical discussion we refer to an accompanying paper in the main journal (Hünsch & Schmitt 1998).

We further note that a similar catalogue of all RASS-detected bright OB-type stars (irrespective of luminosity class) has already been published by Berghöfer et al. (1996).

2. RASS data and detection of late-type stars

2.1. The ROSAT all-sky survey (RASS)

During the first half year, the ROSAT observatory carried out the first all-sky survey with an imaging X-ray telescope. The whole sky was scanned along great circles perpendicular to the direction to the Sun. Because of the Earth's motion around the Sun, the plane of these circles slowly rotated around an axis through the ecliptic poles, thus covering the whole sphere within 6 months. Each point of the sky was observed several times as the scan paths of 2 degrees width (i.e., the field of view of the PSPC detector) progressed along the ecliptic. Therefore, the data of any particular source consist of a number of "snapshots" of up to 30 s duration, separated by the orbital period of the satellite (≈ 90 min) and distributed over an interval of at least 2 days. Towards the ecliptic poles, the cumulative exposure time increases due to the larger number of scans covering a particular position. Depending on the ecliptic latitude (and down-time due to radiation belts of the Earth), the effective exposure time varies between ~ 100 s and $\sim 40\,000$ s (at the poles), with typical values of ~ 400 s on the ecliptic. Given a typical energy-conversion factor for soft sources of $6 \cdot 10^{-12}$ erg cts $^{-1}$ cm $^{-2}$ (cf. Sect. 2.4) the typical detection limit of RASS observations (i.e., ≈ 0.015 cts s $^{-1}$) amounts to $f_x \approx 10^{-13}$ erg cm $^{-2}$ s $^{-1}$. For a more detailed description of the RASS we refer to Voges (1992) and Belloni et al. (1994). Details of the ROSAT observatory in general can be found in Trümper (1983) and Trümper et al. (1991), the PSPC detector used during the RASS is described by Pfeffermann et al. (1986).

The source detection was performed by means of a maximum likelihood algorithm (Cruddace et al. 1988) in the course of the standard analysis software system (SASS; Voges et al. 1992). The significance of an X-ray source is expressed by the likelihood $Li = -\ln(1 - P)$, where P is the probability of existence; e.g., a likelihood of $Li = 7$ corresponds to a source existence likelihood

of 99.9%. The result of the SASS is a comprehensive list of several 10^4 sources, each source described by the sky position in RA and Dec., its source detection likelihood, count rate, hardness ratio, extent, and corresponding errors. The data for the brighter X-ray sources have recently been released as the ROSAT All-sky Survey Bright Source Catalogue (Voges et al. 1996b), which contains sources with Likelihood ≥ 15 and count rate larger than 0.05 s $^{-1}$, that have at least 15 photons.

2.2. Selection of stars

We used the Bright Star Catalogue (BSC; Hoffleit & Warren 1991) as input sample for our search of X-ray bright late-type giants. Specifically, we selected the stars according to their spectral classification, i.e., all stars of spectral types A, F, G, K, M, and C and luminosity classes I, II, III or intermediate classes (including III-IV). We further included those stars without MK spectral classification but with the old Harvard prefix "g", and we also included all composite-spectrum stars with at least one component being of the abovementioned kind. Since the BSC is complete down to apparent visual magnitude ~ 6.2 and has a rather sharp cut-off at $V \approx 6.5 \dots 7.0$, the input sample forms a well defined (optically) flux-limited sample of stars. Given that stars of luminosity class III (or brighter) are normally absolutely brighter than $M_V \approx +1.5$, nearly all giants within a space volume of about 100 pc radius around the Sun are included in the BSC. In total, our input sample contains 3839 stars.

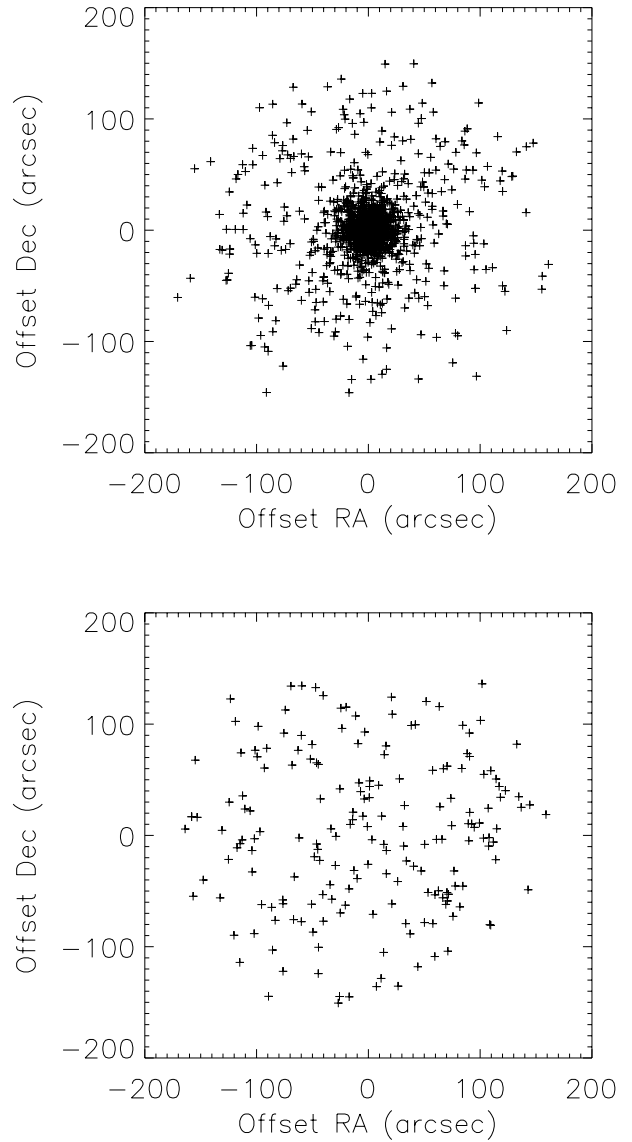
Since about 1 percent of the sky was not included by the RASS, a few BSC stars are not covered by X-ray observations. Those stars with less than 50 s exposure time are listed in Table 1.

2.3. Matches between input stars and RASS-sources

Our aim was to find X-ray sources detected in the RASS close to the positions of the input sample stars defined in the previous subsection. In the first step, we extracted all X-ray sources with a likelihood of ≥ 7 in a square box of 4×4 arcminutes dimension centered on the position of *any* (i.e., 9110) BSC stars. To find out to what distance from the optically selected input positions an X-ray source can reliably attributed to a star, we proceeded as follows: We first constructed a sample of 10 000 random sky positions by means of a Monte Carlo simulation. That sample was subjected to the same match procedure as the 9110 BSC positions. The two-dimensional distribution of the offsets in right ascension and declination between optical and X-ray positions is shown in Fig. 1 for both samples. The corresponding histogram of the offsets (in arcseconds) is plotted in Fig. 2, where the number of matches in each distance interval is normalized to the corresponding annular area, and where a correction factor due to the different numbers of input positions (i.e., 9110 vs. 10 000)

Table 1. Stars of the input sample with less than 50 s exposure time or which are located in the region of the X-ray bright Vela supernova remnant

HR	Name	Sp. type	V
276		G8III	6.32
437	η Psc	G7IIIa	3.62
527		G9III	5.91
731	27 Ari	G5III-IV	6.23
904	7 Eri	M1III	6.11
935		M3III	5.27
959		K1III	6.15
1195		G9II-III	4.17
1285		K0III	6.59
1316		K3-4III	6.71
2851	η CMi	F0III	5.25
2864	6 CMi	K1+III Ba0.4	4.54
2917		K2III	6.76
2955		G8III	6.19
2965		M2IIIab	5.77
2967		M3II-III	5.56
2974		G20-Ia	6.56
2995		G6/8III	6.89
3095	1 Cnc	K3+III	5.78
3376		K0III	6.28
3390		K3III	6.24
3426		A6II	4.14
3444		M0III	5.71
3445		F3Ia	3.84
3452		A5II	4.77
3461	δ Cnc	K0III-IIIb	3.94
3477		G5III	4.07
3487		A1III	3.91
3496		F2Iab	5.75
3520		A2III	4.93
3534		G8III+A3-5V	6.42
3978		K1III	6.52
4007		M3III	6.40
4128		M2IIIe	6.43
4538		G6Ib	4.97
4704	ζ^1 Mus	K0III	5.74
4972		A8II-III	6.33
5122		K1III	6.42
5124		G5Ib	6.01
5251		G8-K0III	5.91
5362		G8III	5.56
5419		K1III	5.97
6076		K5III	6.29
6078		K4III	5.94
7069	111 Her	A5III	4.36
7203		G6III	6.05
7217	\omicron Sgr	G9IIIb	3.77
7370		K4III	5.69
7388		K0-III	6.13
7434		K0III	6.18
7536	δ Sge	M2II+A0V	3.82
7635	γ Sge	M0-III	3.47
7811		G6III	5.66
7813		K0III	6.41
7886		M6III	6.25
7903		A0III	6.08
7913	β Pav	A7III	3.42
7934	σ Pav	K0III	5.41
7941		M5II-III	6.38
7968	ι Ind	K1II-III	5.05
8401	30 Aqr	K0III	5.54
8618	40 Peg	G8II	5.82
8660	45 Peg	gG6	6.25
8929		K1III	6.02
9036	φ Peg	M2.5IIIb	5.08

**Fig. 1.** Distribution of offsets in RA and Dec between optical and X-ray position for matches of RASS sources with the whole BSC star sample (top) and with 10 000 random sky positions (bottom)

was applied. It is evident that for the BSC input sample the number of matches is strongly decreasing towards larger offset values, hence the vast majority of the obtained matches must be real. On the contrary, the similar number of matches for artificial sky positions is approximately independent of the offset distance (as expected), and has a more or less constant value of $\approx 2.63 \cdot 10^{-3}$ matches per square arcsecond. We further note that at an offset of ≈ 90 arcseconds the number of artificial matches is about half the number of actual matches with BSC stars. That means, at that offset the (differential) probability of correctly identifying a BSC star with an X-ray source is about 50%.

Therefore, we chose 90 arcseconds as cut-off match distance between optical and X-ray position, up to which we attribute an X-ray source to a nearby BSC star.

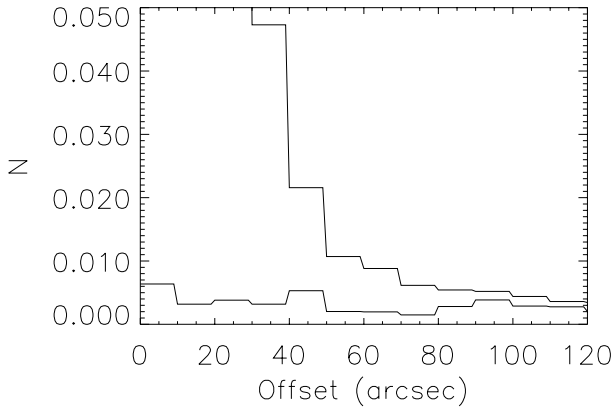


Fig. 2. Histogram of offsets for the BSC star sample (upper line) and the random positions (lower line). The y -axis is given in numbers of matches within a given offset interval, divided by the area of the corresponding annulus

For about 200 X-ray sources extracted in this way and not included in the Bright Source Catalogue (Voges et al. 1996b), we checked the X-ray images by eye for reality. Specifically, we rejected photon distributions that are significantly contaminated by nearby strong sources or that are obviously extended. In questionable cases, we ran the standard source detection algorithm of EXSAS on the source images in different passbands and decided on the basis of the results which sources to retain in our final catalogue.

Confining now attention to the 3839 BSC positions identified with late-type giants and supergiants, we detected X-ray emission from 450 stars, i.e., the average detection rate is 11.7%. Since the total search area around these 3839 stars is $3839 \cdot \pi \cdot (1.5')^2 = 7.54 \square^\circ = 0.018\%$ of the sphere, and the total number of RASS sources amounts to $\sim 150\,000$, we would expect 27.4 chance coincidences of late-type giants or supergiants with background (or foreground) X-ray sources (i.e., 6% of our detected sources). If we consider a maximum offset of 60 arcseconds, this would be even reduced to 12.2 chance coincidences. At least for one case, HR 4289, this has been verified (Hünsch et al. 1996b).

2.4. Determination of X-ray fluxes

The conversion of count rates (CR) into X-ray fluxes is generally performed by application of an energy-conversion-factor (ECF):

$$f_x = \text{ECF} \cdot \text{CR}. \quad (1)$$

ECF depends on both the underlying X-ray spectrum of the source and the amount of interstellar hydrogen absorption. As the source spectrum can be assumed to be thermal emission from an optically thin plasma in the case of late-type stars, the main determining parameter is the temperature of the plasma. However, in addition to the general problems of determining spectral parameters from low-energy-resolution proportional counter measurements, the detailed analysis of X-ray spectra requires quite a large number of photons, i.e., bright sources or long exposure times. For most of the sources in our catalogue, these requirements are not fulfilled, thus their coronal temperatures are unknown. Moreover, information on the interstellar hydrogen column density is also lacking for most of the stars. For late-type stars, colour excesses are difficult to measure due to the large intrinsic scatter of the colour indices. On the other hand, giants are intrinsically bright objects, on average they are far away and the amount of interstellar absorption cannot be neglected in most cases.

Fortunately, a rough information on the energy distribution in the X-ray range is provided by the hardness ratio.

$$hr = \frac{H - S}{H + S}, \quad (2)$$

where H and S denote the source counts in the hard (0.5 – 2.0 keV) and soft (0.1 – 0.4 keV) passbands of ROSAT. The hardness ratio is an “X-ray colour” that is influenced by both the plasma temperature and the hydrogen column density. Hünsch et al. (1996a) analyzed several PSPC pulse-height spectra of nearby giants and find from modelling the observed energy distributions by isothermal or two-temperature-component Raymond-Smith (1977) models a linear relation

$$\text{ECF} = (5.30 \cdot hr + 8.7) \cdot 10^{-12} \text{ erg cm}^{-2} \text{ cts}^{-1}. \quad (3)$$

Note that Schmitt et al. (1995) find a very similar relation for late-type main-sequence stars.

Since the SASS source detection was separately performed in both passbands, and since most of our X-ray sources were detected in both bands, the hardness ratios can be determined for most stars, although in some cases with quite large errors. In a few cases, where the sources were not detected in the soft passband, we set $hr = +1.0$ by definition. The error in the hardness ratio is given by

$$\sigma_{hr} = 2(S + H)^{-1.5} \cdot \sqrt{S \cdot H}. \quad (4)$$

From the hardness ratios, we calculated individual energy-conversion-factors, which cover a range of $\text{ECF} = 4 \dots 14 \cdot 10^{-12} \text{ erg cts}^{-1} \text{ cm}^{-2}$. We refrain from estimating individual errors for f_x since the error in ECF is very difficult to quantify. In general, we estimate the error to be within a factor of two for the weaker sources and less for the brighter sources.

Since the apparent flux f_x depends on the distance, a more characteristic measure would be the X-ray luminosity L_x . However, reliable distance measurements from parallaxes exist only for a minority of our sample stars. Spectroscopic parallaxes from luminosity classes are quite uncertain and absolute magnitudes from the Wilson-Bappu effect exist only for part of the stars brighter than $V \approx 5$. Therefore, we did not calculate individual X-ray luminosities. A distance-independent measure of the level of X-ray emission is the ratio of X-ray to bolometric flux. We calculated bolometric fluxes from the relation

$$f_{\text{bol}} = 2.7 \cdot 10^{-5} \cdot 10^{-\frac{m_{\text{bol}}}{2.5}} \text{ erg cm}^{-2} \text{ s}^{-1}, \quad (5)$$

where the apparent bolometric magnitude is given by $m_{\text{bol}} = V + \text{B.C.}$ The bolometric corrections B.C. were taken from the tables of Schmidt-Kaler (1982) as given in the Landolt-Börnstein, by interpolating the values in colour index $B - V$ and luminosity class whenever necessary. For the M-type stars, we used the spectral type instead of the colour index due to the weak dependence of B.C. on $B - V$.

3. The catalogue

The table contains optical and X-ray data of all 450 detected late-type giants and supergiants including A-type stars listed in the BSC.

The columns of the table contain the following information:

- Column 1: HR number (BSC)
- Column 2: HD number
- Column 3: the star's name (Bayer or Flamsteed designation)
- Column 4: V magnitude (from BSC)
- Column 5: $B - V$ colour index (from BSC)
- Column 6: MK spectral classification (from BSC)
- Column 7: binary flag; S: single star, VB: visual binary (if a companion within 90 arcseconds distance is known), SB: spectroscopic binary (as given in the BSC), RS: RS CVn system (usually also SB), B: other binary (composite spectrum), CV: cataclysmic companion (HR 4765 = 4 Dra), Symb: symbiotic star (HR 8992 = R Aqr)
- Column 8: effective exposure time in seconds
- Column 9: mean PSPC count rate in counts per second
- Column 10: error of PSPC count rate
- Column 11: likelihood of existence (cf. Sect. 2.1)
- Column 12: offset in arcseconds between optical and X-ray position
- Column 13: hardness ratio $hr = (H - S)/(H + S)$ (cf. Sect. 2.4)
- Column 14: error of hardness ratio
- Column 15: apparent X-ray flux (0.1 – 2.4 keV) in

$10^{-14} \text{ erg cm}^{-2} \text{ s}^{-1}$ (see Sect. 2.4)

Column 16: logarithm of X-ray to bolometric flux ratio (see Sect. 2.4).

Acknowledgements. The ROSAT project is supported by the Bundesministerium für Bildung, Forschung und Technologie (BMBF/DARA) and the Max-Planck-Gesellschaft (MPG). We would like to thank our colleagues from the MPE ROSAT group, especially T. Berghöfer, for their support. MH acknowledges the hospitality of the MPE during his stay in Garching.

References

- Ayres T.R., Linsky J.L., Vaiana G.S., Golub L., Rosner R., 1981, ApJ 250, 293
- Belloni T., Hasinger G., Izzo C., 1994, A&A 283, 1037
- Berghöfer T.W., Schmitt J.H.M.M., Cassinelli J.P., 1996, A&AS 118, 481
- Cruddace R.G., Hasinger G.R., Schmitt J.H.M.M., 1988, The application of a maximum likelihood analysis to detection of sources in the ROSAT data, in: Murtagh F., Heck A. (eds.) Astronomy from Large Databases, ESO Conf. Workshop Proc. 28, 177
- Haisch B.M., Schmitt J.H.M.M., Rosso C., 1991, ApJ 383, L15
- Haisch B.M., Schmitt J.H.M.M., Fabian A.C., 1992, Nat 360, 239
- Hoffleit D.E., Warren W.H.jr., 1991, The Bright Star Catalogue, 5th Rev. Ed., Yale Univ. Obs., New Haven
- Hünsch M., Schmitt J.H.M.M., 1998, A&A (in preparation)
- Hünsch M., Schröder K.-P., 1996, A&A 309, L51
- Hünsch M., Schmitt J.H.M.M., Schröder K.-P., Reimers D., 1996a, A&A 310, 801
- Hünsch M., Reimers D., Schmitt J.H.M.M., 1996b, A&A 313, 755
- Linsky J.L., Haisch B.M., 1979, ApJ 229, L27
- Maggio A., Vaiana G.S., Haisch B.M., et al., 1990, ApJ 348, 253
- Pallavicini R., Golub L., Rosner R., et al., 1981, ApJ 248, 279
- Pfeffermann E., Briel U.G., Hippmann U., et al., 1986, Proc. SPIE 733, 519
- Raymond J., Smith B.W., 1977, ApJS 35, 419
- Reimers D., Hünsch M., Schmitt J.H.M.M., Toussaint F., 1996, A&A 310, 813
- Schmidt-Kaler T., 1982, in: Voigt H.H., Schaifers K. (eds.) Landolt-Börnstein VI, 2b. Springer, Heidelberg
- Schmitt J.H.M.M., 1997, A&A 318, 215
- Schmitt J.H.M.M., Fleming T.A., Giampapa M.S., 1995, ApJ 450, 392
- Trümper J., 1983, Adv. Space Res. 2, 241
- Trümper J., et al., 1991, Nat 349, 579
- Vaiana G.S., Cassinelli J.P., Fabbiano G., et al., 1981, ApJ 244, 163
- Voges W., 1992, in: Proc. of the ISY Conf. "Space Science", ESA ISY-3, ESA Publ., p. 9
- Voges W., et al., 1992, in: Proc. of the ISY Conf. "Space Science", ESA ISY-3, ESA Publ., p. 223
- Voges W., et al., 1996a, MPE Report 263, 637
- Voges W., et al., 1996b, IAUC 6420